# COVID-19 Detection on CT Scans Using Local Binary Pattern and Deep Learning

Sertan Serte[1(✉)] and Fadi Al-Turjman[2]

[1] Near East University, North Cyprus via Mersin 10, Nicosia, Turkey
sertan.serte@neu.edu.tr
[2] Research Center for AI and IoT, Near East University, Mersin 10, Nicosia, Turkey
fadi.alturjman@neu.edu.tr

**Abstract.** X-ray and CT scans show lungs, and images can be used to differentiate positive and negative cases. Analyzing these scans using an artificial intelligent method might provide fast and accurate COVID-19 detection. In this paper, a local binary pattern based deep learning method is proposed for the detection of COVID-19 infection on CT Scans. The proposed technique generates local binary pattern (LBP) representations of the CT scans, and then these representations are modeled using fine-tuned models. The fine-tuned models are AlexNet, VGG, ResNet-18, ResNet-50, MobileNetV2, and DensNet-121. We show that the proposed local binary pattern based deep learning model provides higher performance than classic deep learning models for COVID-19 detection. The classification performance of the method provides 90% AUC value for COVID-19 detection.

**Keywords:** Convolutional neural networks · Deep learning · Local binary pattern (LBP) · COVID-19

## 1 Introduction

A new respiratory disease, Coronavirus, appeared in Wuhan China in 2019, [27]. Coronavirus [14] is known as viral pneumonia, and this viral pneumonia can be group into COVID-19, SARS, and MERS. Bacterial and fungus types of pneumonia are non-COVID-19 pneumonia types. Streptococcus is a type of bacterial pneumonia, while pneumocystis is a type of fungus pneumonia.

Currently, people are catching this disease from each other, and there is no vaccine for COVID-19 disease. The only wave of avoiding infection is to isolate infected people from healthy ones. Therefore, regular COVID-19 tests are necessary for the identification of infection on people to separate them. Transcription-polymerase chain reaction (RT-PCR) tests mainly allow to detect people with COVID-19 in hospitals.

Computed tomography scan (CT scan) and X-ray images are alternative diagnostic tools for detecting COVID-19. Doctors image lungs and look for signs of COVID-19 deformations on the CT or X-Ray images. This process requires a certain amount of time for correct pneumonia type classification.


S. Paiva et al. (Eds.): SmartCity360° 2020, LNICST 372, pp. 101–107, 2021.
https://doi.org/10.1007/978-3-030-76063-2_7

However, convolutional neural networks (CNNs) might be used instead of or in conjunction with the doctors for faster and better diagnosis of COVID-19 on CT scans. CNNs include AlexNet [11], GoogleNet [25], VGG [24], MobileNetV2 [16], ResNet [6] and DenseNet [9]. These models have provided the classification of 1,000 objects in the ImageNet dataset [3]. The performance results show that these models are close to human-level object-level accuracy. These models also result in high classification performance in medical image classification. Recent studies in [10,17,20,22,23] used CNNs to model skin lesion detection. The authors [18,19,21] also proposed to detect eye disease on funds images.

The proposed deep learning model (Fig. 1) is different than previous works [12,27]. In this paper, a local binary pattern based deep learning model is proposed to detect COVID-19 on CT-scans. The proposed approach builds on obtaining local binary pattern representations [8,26] of CT scans, and then these LBP structures are used as inputs to the fine-turned models for COVID-19 classification. LBP allowed to creates local forms of COVID-19 related regions. Both image and structure-based models are evaluated on COVID19-CT dataset. Results show that local binary pattern based models outperform the classic image-based CNN models. The main novelties of this work are:

1. A new local binary pattern based deep learning model is proposed for COVID-19 detection on CT scans.
2. The ResNet18 convolutional neural network is proposed to model local binary pattern features of diagnosis of COVID-19 on CT exams.
3. The performance comparisons provide model evaluation for COVID-19 classification.

The organization of this paper is as follows. First, the information about recent works is given. Second, the proposed approach is introduced. Furthermore, the proposed deep learning method is presented. In addition, the performances of classic and local binary pattern based models are compared.

## 2 Related Work

Combining CNN and a Generative Adversarial Network (GAN) models is another way of achieving data-efficient models. GAN models [4,15,27,28], are known as creating synthetic images from a given set of images. This model architecture includes generator and discriminator networks. The generator is responsible for synthetic image generating while the discriminator compares real and synthetic images during this process. A review [28] reports all proposed GAN models.

Mei et al. [13] proposed to use the Resnet-18 convolutional neural network in conjunction with support vector machines for COVID-19 detection. In this work, the CNN model allows prediction on the CT image, while SVM provides COVID-19 prediction on non-image data. Authors combine ResNet-18 and SVM outputs to detect COVID-19.

Harmon et al. [5] utilized DensNet-121 deep learning architecture for classification of COVID-19 and pneumonia. The proposed method train and tested on a multi dataset for performance evaluation.

Bhandary et al. [1] use AlexNet in conjunction with support vector machines to classify COVID-19 and cancer on X-Ray and CT Scans. Authors also compare the SVM based Alexnet with AlexNet, VGG16, VGG19, and ResNet50.

Butt et al. [2] use ResNet-18 deep learning model for the classifying COVID-19, viral pneumonia, and normal CT scans. This method builds on creating 3D volumes of the CT scans and then extracting paths from these regions. Then these images were used as inputs to the ResNet-18 model for differentiating COVID-19, viral pneumonia, and normal CT scans.

## 3 Method

In the trainig part, image based fine-tuned AlexNet, VGG, ResNet-18, ResNet-50, MobileNetV2, and DensNet-121 models generated. A set of CT scans are augmented and used as inputs to the fined-tuned models for modeling COVID-19.

The structure-based fine-tuned LAlexNet, LVGG, LResNet-18, LResNet-50, LMobileNetV2, and LDensNet-121 models are also generated. A set of CT scans are transformed into LBP images [8,26]. Then transformed images are augmented and used as inputs to the fined-tuned models for training.

In the testing part, a test CT scan and LBP representation used as inputs to the image and structured based models, respectively. Each of the models provides output probabilities of COVID-19 and non-COVID19 predictions (Table 3).

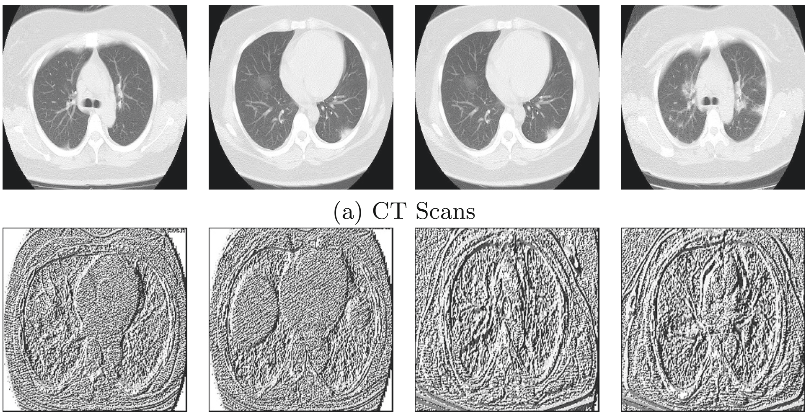

(a) CT Scans

(b) LBP Images

**Fig. 1.** Sample images from each dataset

**Table 1.** Total number of images in the datasets

| CT-Scan | Dataset | Train | Test |
|---|---|---|---|
| COVID-19 | COVID19-CT | 324 | 40 |
| Normal | COVID19-CT | 293 | 37 |

**Table 2.** Total number of images in the datasets

| Data | CT-Scan | Dataset | Train | Test |
|---|---|---|---|---|
| Image | COVID-19 | COVID19-CT | 1393 | 40 |
| Image | Normal | COVID19-CT | 1672 | 37 |
| LBP | COVID-19 | COVID19-CT | 1393 | 40 |
| LBP | Normal | COVID19-CT | 1672 | 37 |

### 3.1 COVID19-CT Dataset

COVID19-CT dataset [7] includes 349 COVID-19 and 397 healthy CT scans. Figure 1 also shows the sample images from this dataset. The authors collected these CT-Scans from medRxiv3 and bioRxiv4 preprints. Images in the preprints show the COVID-19 finding on the images. Some of these findings can be seen clearly in the images.

### 3.2 Augmented Datasets

The fine-tuned models allow modeling COVID-19 and non-COVID-19 disease on the dataset. Since the available imaged are small in the dataset, the CT images are augmented, and then these images are used for model training. The CT scans of the training set are rotated to obtain an augmented dataset. Table 2 shows the number of augmented CT scans for COVID19-CT dataset. First, the dataset is split into training and testing sets. Then augmentation is performed on training images.

### 3.3 Model Generations

The fine-tuned models are generated for image and local binary pattern based deep learning methods. These fined-tuned models are the AlexNet, VGG, ResNet-18, ResNet-50, MobileNetV2, and DensNet-121.

All these models are pre-trained on the ImageNet dataset and the re-trained on CT scans and LBP images. The images are resized to $256 \times 256$ RGB images, and then these images are used as inputs to the CNN models. The $224 \times 224 \times 3$ random crops are extracted. The parameters of the convolutional layers are frozen, and only fully connected layers are estimated. To conclude, the proposed data-efficient models are fine-tuned for CT scans and LBP images of COVID-19 and non-COVID-19.

**Table 3.** Performance comparisons of single CNN models on COVID19-CT and Mosmed datasets.

| Network | Data | AUC | ACC | SE | SP |
|---|---|---|---|---|---|
| AlexNet | Image | 0.60 | 0.67 | 0.72 | 0.64 |
| MobileNetV2 | Image | 0.71 | 0.73 | 0.82 | 0.69 |
| Resnet18 | Image | 0.77 | 0.75 | 0.83 | 0.71 |
| Resnet50 | Image | 0.71 | 0.77 | 0.86 | 0.72 |
| Vgg | Image | 0.65 | 0.75 | 0.86 | 0.70 |
| Densenet121 | Image | 0.70 | 0.74 | 0.87 | 0.69 |
| LResnet18 | LBP | **0.90** | 0.65 | 0.77 | 0.62 |
| LResnet50 | LBP | 0.69 | 0.68 | 0.81 | 0.64 |
| LVgg | LBP | 0.63 | 0.67 | 0.80 | 0.63 |
| LAlexNet | LBP | 0.44 | 0.73 | 0.79 | 0.70 |
| LDensenet121 | LBP | 0.45 | 0.65 | 0.71 | 0.63 |
| LMobileNetV2 | LBP | 0.55 | 0.67 | 0.75 | 0.64 |

## 4 Performance Evaluation

Performance evaluation is performed using metrics as described follows. The area under the receiver operating characteristic (ROC) curve (AUC), accuracy (ACC), sensitivity (SE), and specificity (SP) performance merits are used to test the accuracy of the methods. We can describe accuracy, sensitivity, and specificity as:

$$\text{Accuracy} = \frac{\text{TP+TN}}{\text{TP+TN+FP+FN}} \tag{1}$$

$$\text{Sensetivity} = \frac{\text{TP}}{\text{TP+FN}} \tag{2}$$

$$\text{Specificity} = \frac{\text{TN}}{\text{TN+FP}} \tag{3}$$

where true positive, positive, true negative, false positive, and false negative are denoted as TP, TN, FP, and FN, respectively.

### 4.1 Image-Based Deep Learning Method

Table 3 reports the performances the AlexNet, VGG, ResNet-18, ResNet-50, MobileNetV2, and DensNet-121 deep learning models. These models only build on augmented data of the CT scans. These models are evaluated for on the COVID19-CT dataset.

### 4.2 Proposed Structure-Based Method

The performances of the proposed structure-based deep learning models are also evaluated in Table 3. Fine-tuned models build on LBP images of the CT scans. These fine-tuned models are AlexNet, VGG, ResNet-18, ResNet-50, MobileNetV2, and DensNet-121.

## 5 Conclusion

The image and local binary pattern based deep learning methods are proposed for COVID-19 detection on CT scans. The proposed methods build on both CT scans and LBP images of COVID19-CT dataset. This novel method allowed structuring available CT scans using LBP method. The fine-tuned The AlexNet, VGG, ResNet-18, ResNet-50, MobileNetV2, and DensNet-121 image-based models are generated. The LAlexNet, LVGG, LResNet-18, LResNet-50, LMobileNetV2, and LDensNet-121 LBP data based models also created. The results show that the proposed unified image and LBP-based model outperform image and structure-based models.

## References

1. Bhandary, A., et al.: Deep-learning framework to detect lung abnormality - a study with chest x-ray and lung CT scan images. Pattern Recogn. Lett. **129**, 271–278 (2020)
2. Butt, C., Gill, J., Chun, D., Babu, B.A.: Deep learning system to screen coronavirus disease 2019 pneumonia. Appl. Intell. 1–7 (2020)
3. Deng, J., Dong, W., Socher, R., Li, L.J., Li, K., Fei-Fei, L.: ImageNet: a large-scale hierarchical image database. In: CVPR09 (2009)
4. Goodfellow, I.J., Shlens, J., Szegedy, C.: Explaining and harnessing adversarial examples (2014)
5. Harmon, S.A., Sanford, T.H., Xu, S., Turkbey, E.B., et al.: Artificial intelligence for the detection of COVID-19 pneumonia on chest CT using multinational datasets. Nat. Commun. **11**, 4080 (2020)
6. He, K., Zhang, X., Ren, S., Sun, J.: Deep residual learning for image recognition. In: 2016 IEEE Conference on Computer Vision and Pattern Recognition (CVPR), pp. 770–778 (2016)
7. He, X., et al.: Sample-efficient deep learning for COVID-19 diagnosis based on CT scans. medrxiv (2020)
8. Huang, D., Shan, C., Ardabilian, M., Wang, Y., Chen, L.: Local binary patterns and its application to facial image analysis: a survey. IEEE Trans. Syst. Man Cybernet. Part C (Appl. Rev.) **41**(6), 765–781 (2011)
9. Huang, G., Liu, Z., van der Maaten, L., Weinberger, K.Q.: Densely connected convolutional networks (2016)
10. Kaymak, S., Esmaili, P., Serener, A.: Deep learning for two-step classification of malignant pigmented skin lesions. In: 2018 14th Symposium on Neural Networks and Applications (NEUREL), pp. 1–6 (2018)

11. Krizhevsky, A., Sutskever, I., Hinton, G.E.: Imagenet classification with deep convolutional neural networks. In: Pereira, F., Burges, C.J.C., Bottou, L., Weinberger, K.Q. (eds.) Advances in Neural Information Processing Systems, vol. 25, pp. 1097–1105 (2012)
12. Loey, M., Smarandache, F., Khalifa, N.E.: Within the lack of chest COVID-19 x-ray dataset: a novel detection model based on GAN and deep transfer learning. Symmetry **12**, 651 (2020)
13. Mei, X., et al.: Artificial intelligence-enabled rapid diagnosis of patients with COVID-19. Nat. Med. **26**, 1–5 (2020). https://doi.org/10.1038/s41591-020-0931-3
14. Pereira, R.M., Bertolini, D., Teixeira, L.O., Silla, C.N., Costa, Y.M.: COVID-19 identification in chest x-ray images on flat and hierarchical classification scenarios. Comput. Methods Programs Biomed. **194** (2020)
15. Radford, A., Metz, L., Chintala, S.: Unsupervised representation learning with deep convolutional generative adversarial networks (2015)
16. Sandler, M., Howard, A., Zhu, M., Zhmoginov, A., Chen, L.: Mobilenetv 2: inverted residuals and linear bottlenecks. In: 2018 IEEE/CVF Conference on Computer Vision and Pattern Recognition, pp. 4510–4520 (2018)
17. Serener, A., Serte, S.: Keratinocyte carcinoma detection via convolutional neural networks. In: 2019 3rd International Symposium on Multidisciplinary Studies and Innovative Technologies (ISMSIT), pp. 1–5 (2019)
18. Serener, A., Serte, S.: Transfer learning for early and advanced glaucoma detection with convolutional neural networks. In: 2019 Medical Technologies Congress (TIPTEKNO), pp. 1–4 (2019)
19. Serener, A., Serte, S.: Geographic variation and ethnicity in diabetic retinopathy detection via deeplearning. Turk. J. Electr. Eng. Comput. Sci. **28**, 664–678 (2020)
20. Serte, S., Demirel, H.: Wavelet-based deep learning for skin lesion classification. IET Image Proc. **14**(4), 720–726 (2020)
21. Serte, S., Serener, A.: A generalized deep learning model for glaucoma detection. In: 2019 3rd International Symposium on Multidisciplinary Studies and Innovative Technologies (ISMSIT), pp. 1–5 (2019)
22. Serte, S., Demirel, H.: Gabor wavelet-based deep learning for skin lesion classification. Comput. Biol. Med. **113** (2019)
23. Serte, S., Serener, A., Al-Turjman, F.: Deep learning in medical imaging: a brief review. Trans. Emerg. Telecommun. Technol.
24. Simonyan, K., Zisserman, A.: Very deep convolutional networks for large-scale image recognition (2014)
25. Szegedy, C., et al.: Going deeper with convolutions. In: 2015 IEEE Conference on Computer Vision and Pattern Recognition (CVPR), pp. 1–9 (2015)
26. Tuncer, T., Dogan, S., Ozyurt, F.: An automated residual exemplar local binary pattern and iterative relieff based COVID-19 detection method using chest x-ray image. Chemom. Intell. Lab. Syst. **203** (2020)
27. Waheed, A., Goyal, M., Gupta, D., Khanna, A., Al-Turjman, F., Pinheiro, P.R.: Covidgan: data augmentation using auxiliary classifier GAN for improved COVID-19 detection. IEEE Access **8**, 91916–91923 (2020)
28. Yi, X., Walia, E., Babyn, P.: Generative adversarial network in medical imaging: A review. Med. Image Anal. **58** (2019)